# Supplementary Information for:

# Designing Novel Carangiform Fish Robots with Undulating Hair Clip Mechanisms

Zechen Xiong[1, *], Liqi Chen[2], Sarah Li Wilkinson[2], Md Raf E Ul Shougat[1], Hod Lipson[2]

[1]*Ingram School of Engineering, Texas State University, San Marcos, TX 78666, USA*
[2]*Department of Mechanical Engineering, Columbia University, New York, NY 10027, USA.*
[*]*Correspondence: uji21@txstate.edu*

**The PDF file includes:**

Supplementary text
fig. S1 to S6
Captions for movies S1 to S9

**Other Supplementary Material:**

movies S1 to S9
HCM_Theory_1_0.mlx

Measurement of tip bending angles

The experimental bending angles of prestressed HCMs in Fig. 2A and 2B are measured using a 1-Axis Soft Flex Sensor (Bend Labs Inc.) that is connected to the microcontroller of SparkFun Pro nRF52840 Mini (fig. S1).

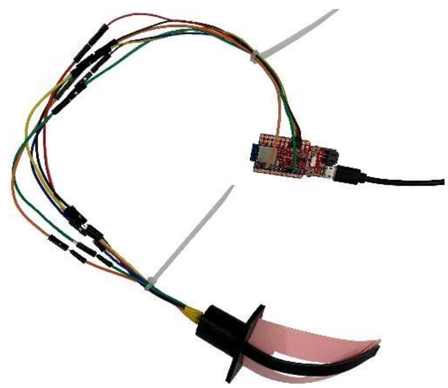

**fig. S1 Electronic setup for the measurement of bending angles for the assembled HCM.**

Fabrication of the fish robots

Both heads of the pneumatic fish robot and the motor-driven fish robot are 3D printed after being modeled in Solidworks. The pneumatic soft bending units are fabricated using the 3D-printed molds (Ultimaker S3, PLA) and cast with Dragon Skin 20 (Smooth-On Inc.), as shown in fig. S2. Plastic glue (Loctite Super Glue) is used to bond the cured silicone rubber bending units to the plastic shims.

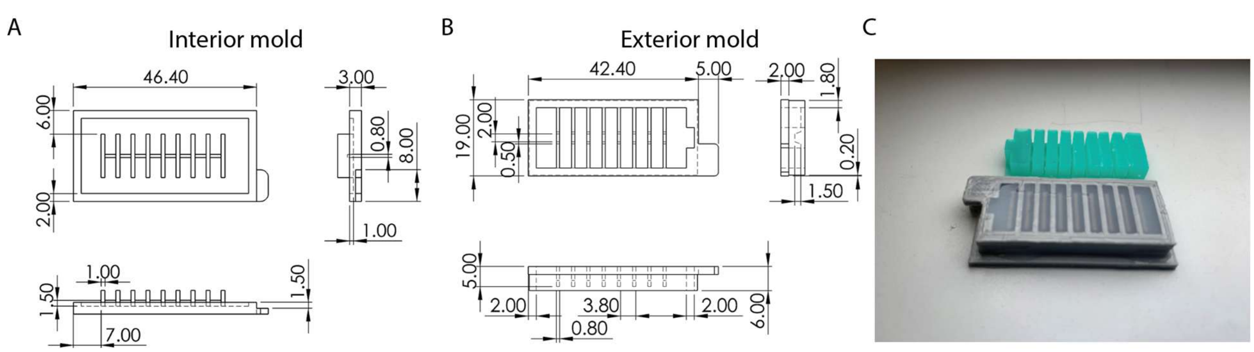


**fig. S2 The fabrication of the pneumatic bending units. (A)** Dimensions (mm) of the interior mold for the pneumatic bending unit. The top, side, and front views are included. **(B)** Dimensions of the exterior mold. **(C)** The cured and curing silicone rubber pneumatic bending units. Both units are made from Dragon Skin 20, and one of them is tinted with dye.

The plastic HCM ribbons are laser-cut (using Thunder Laser Nova51) from color-coded shims (McMaster-Carr, 9513K), and metal HCM ribbons are swater-jetted from stainless steel shim stock sets (McMaster-Carr, 93005K). In the assembly of these HCMs, the extremities of HCMs are pin-locked using press-fit rivets (McMaster-Carr, 97362A) (fig. S3 and Figs. 4 and 5).

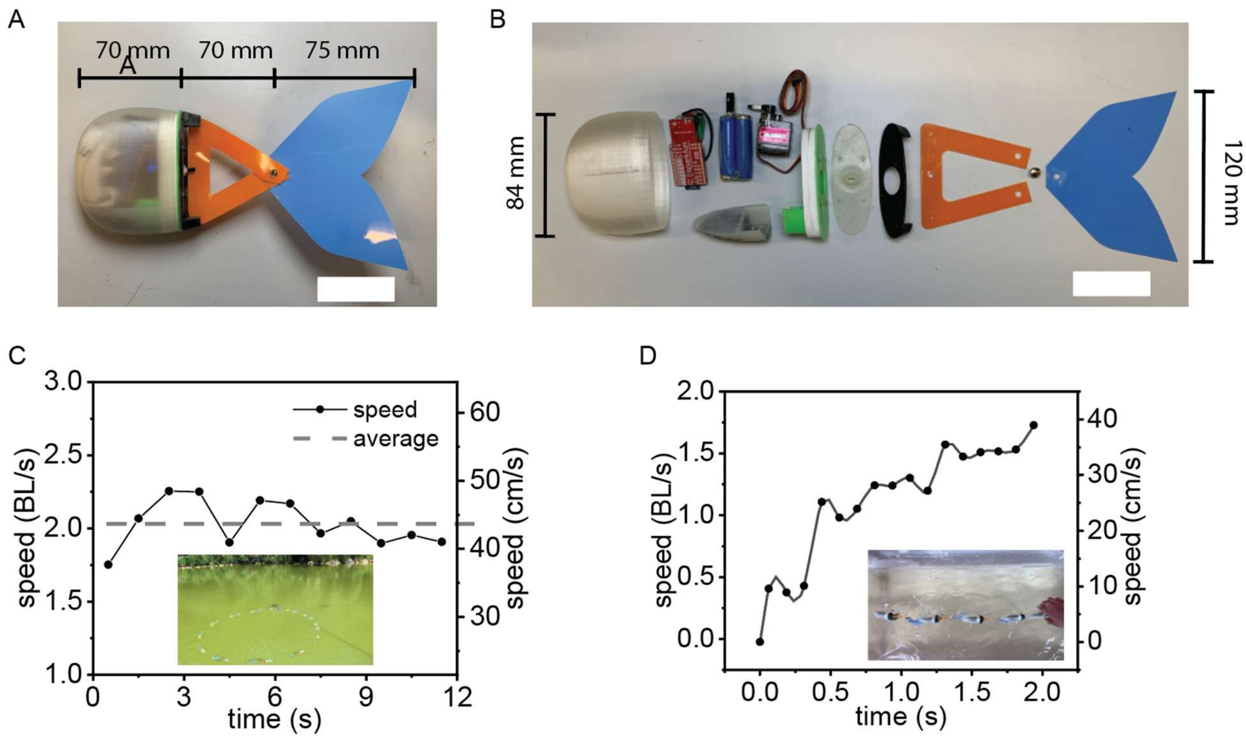


**fig. S3 The motor-driven untethered fish robot and its speed profiles. (A)** and **(B)** The assembly and parts of the robot, respectively. **(C)** and **(D)** The speed profiles of the robot in a lake and in an aquarium tank, respectively. The HCM body of the fish has shape factors $\theta = -23.5°$, and $\gamma_s = 2$. Undulation frequency is 3Hz in both situations. The average cruising speed and starting acceleration measured are 2.03 BL/s or 43.6 cm/s and 20.1 cm/s$^2$.

## Thrust and efficiency

A series of benchtop tests was conducted using an Arduino-based circuit equipped with bending load cells and an INA226 current and power sensor. The experimental setup and corresponding results are shown in fig. S4.

Thrust output peaked at an undulation frequency between 3 and 3.5 Hz, with 3 Hz being the most efficient, yielding a thrust-to-power ratio of 79.46 mN/W. On the other hand, if we define power efficiency as

$$\eta = TU/P$$

where $T$ is the thrust, $U$ the forward velocity, and $P$ the input power, the undulation at 3 Hz achieved an efficiency of 3.89% and a corresponding cost of transport (CoT) of 5.143.

Above 3.5 Hz, thrust decreases due to the MG90s servo's limited snapping frequency, constrained by its maximum spinning speed. However, failed snapping at higher frequencies lowers power consumption (from 3.20 W to 2.93 W in fig. S4B).

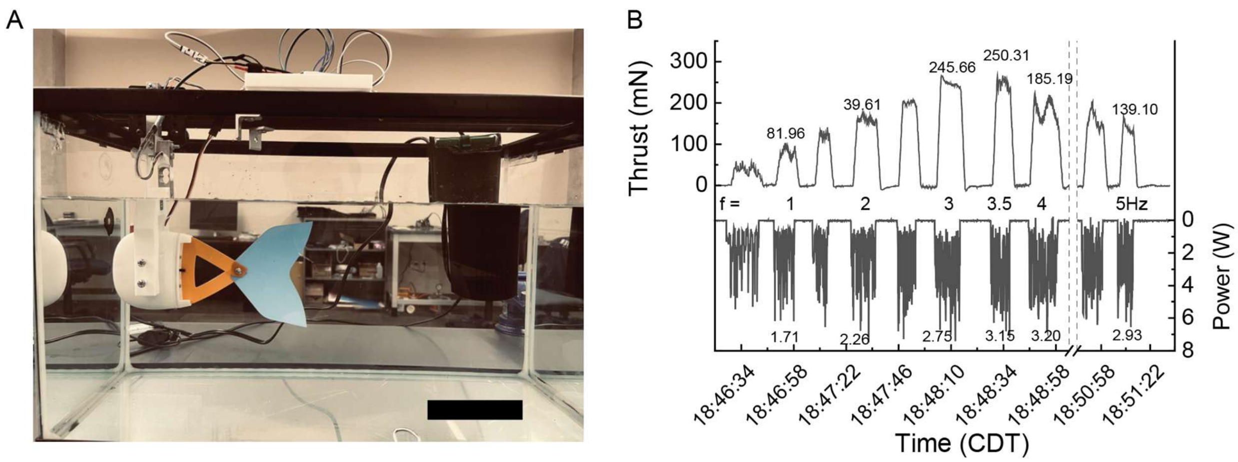


**fig. S4 Benchtop evaluation of servo-driven HCM fish performance. (A)** Experimental setup for measuring thrust and power consumption. The setup includes an Arduino-based circuit, two bending load cells, and an INA226 current/power sensor (scale bar = 10 cm). **(B)** Measured thrust and power consumption as a function of undulation frequency (0.5–5.0 Hz).

<u>Material properties</u>

According to the HCM theory in the manuscript, Young's moduli of the materials of an HCM have a critical influence on its mechanical features. While the modulus of the steel can be estimated to be 200 GPa, the moduli of the PETG color-coded plastic sheet (McMaster-Carr, 9536K) and the silicone rubber (Smooth-On Inc., Dragon Skin 10) are measured via a tensile machine (SUNS, UTM4000), following the guidance of ASTM D882 and ASTM E8/E8M, respectively. Five PETG samples are laser-cut (Thunder Laser Nova51), and three silicone rubber samples are cast from 3D-printed molds (Ultimaker S3, PLA plastic). The process and results are shown in fig. S5. Assuming linear elasticity, the moduli of the PETG plastic sheets (averaged from

5 samples) and Dragon Skin 20 silicone rubber (averaged from 3 samples) are 1.73 GPa and 885 kPa, respectively.

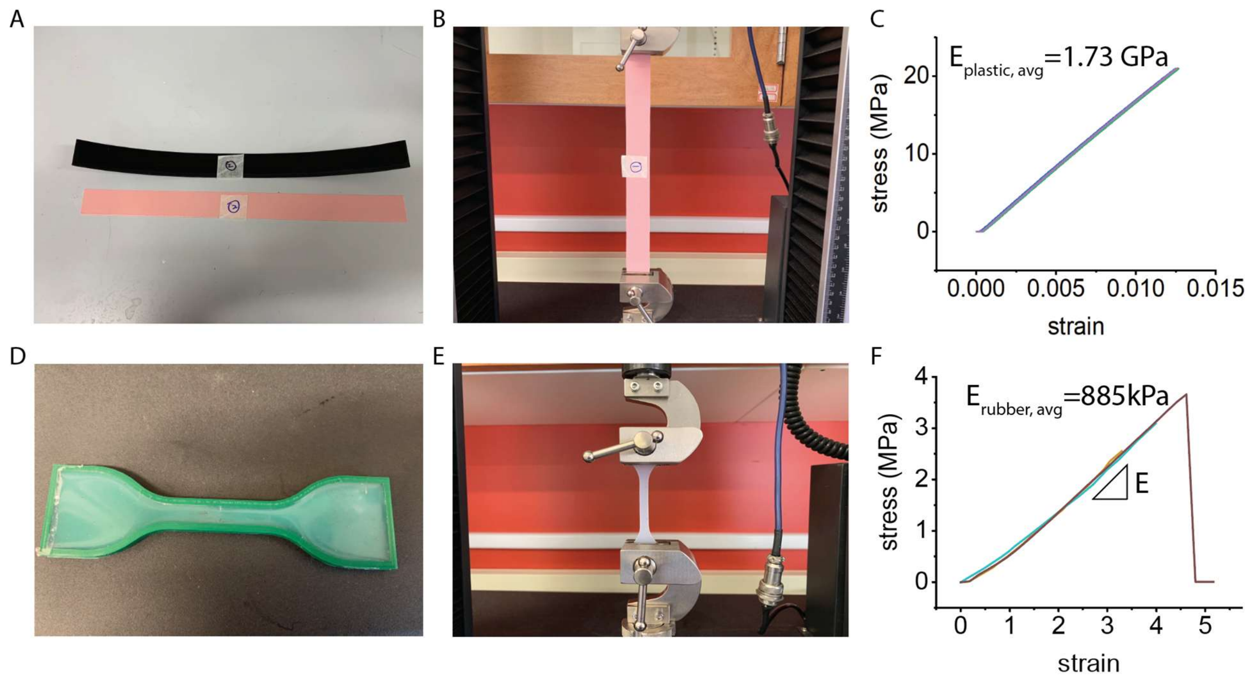


**fig. S5 Measurement of the tensile moduli of PETG and silicone rubber. (A)** Preparation of the PETG plastic samples following ASTM D882. The pink one has a thickness of 0.381mm; the black is 0.254 mm in thickness. **(B)** Tensile test of the PETG samples. **(C)** The stress-strain curves of 5 samples of PETG. An average modulus of 1.73 GPa is calculated from the slope of the curves following ASTM D882. **(D)** Preparation of Dragon Skin 20 silicone rubber following ASTM E8/E8M. **(E)** Tensile test of the silicone rubber samples. **(F)** The stress-strain curves of 3 samples of silicone rubber. An average modulus of 885 kPa is calculated from the straight segment of the curves.

Pneumatic Actuation of the HCM

By gluing pneumatic bending units to the surface of an HCM, we create a bistable fishtail mechanism whose snap-through buckling can be triggered by pumping air into the bending pneumatic networks. The pressure needed for the onset of HCM snapping, which is called critical pressure, is measured with the setup in fig. S6. A quasi-static pressurizing scheme is applied until snap-through, and the critical pressure is measured on HCMs with different values of shape factor $\theta$ yet constant $\gamma_s = 6$. The curve is divided into two linear segments. The linear relation is because the energy barrier of the HCM is proportional to the shape factor $\theta$, according to the theoretical expression of the energy barrier in Eq. (6). The slope of the curve is smaller when $\theta > 0$ than when

$\theta < 0$. This is because the ridges of the soft pneu-nets (fig. S2) will contact and interfere with each other at the rest state when $\theta > 0$ and make the snap-through of the pneumatic HCM easier.

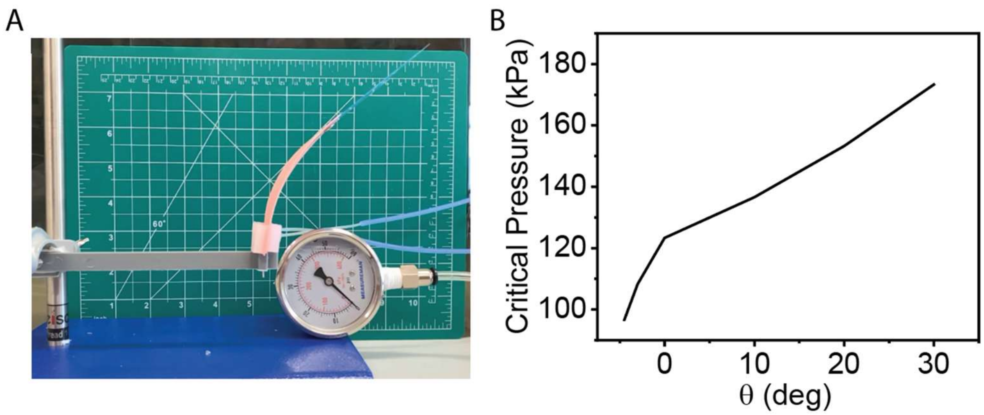


**fig. S6 Measurement of the critical pressure of the pneumatic HCM fishtail. (A)** The setup for measuring the critical pressure of the HCM pneumatic fishtail. **(B)** The critical pressures of the HCM pneumatic fishtail w.r.t $\theta$ when $\gamma_s = 6$. Two near-linear segments are observed.

**Movie captions:**

**movie S1. The assembly of PETG and steel HCMs.** The thickness and shape factors of the PETG plastic HCM ribbon are $t$ = 0.381mm, $\theta$ = 20˚, and $\gamma_s = L_2 / L_1 = 6$, while those of the metal HCM are $t$ = 0.152mm, $\theta$ = 10˚, and $\gamma_s$ = 6

**movie S2. The slo-mo (0.125x) demonstration of the snapping of plastic and metal HCMs.** The PETG plastic HCM snaps in ~40 ms, and the metal HCM in ~16 ms.

**movie S3. The Comparison of real-time swimming of the HCM-driven fish robot and its conventional soft counterpart.** The pneumatic actuation system pressurizes at 150 kPa and 1.3 Hz for both tests. The HCM used in the robot has shape factors $\theta = -3$˚ and $\gamma_s$ = 6.

**movie S4. The Comparison of slo-mo swimming of the HCM-driven fish robot and its conventional soft counterpart.** The movie is filmed at 240 fps.

**movie S5. The high-frequency real-time swinging of the pneumatic HCM fishtail.** The HCM has shape factors $\theta$ = 10˚ and $\gamma_s$ = 6. The pneumatic actuation system pressurizes at ~300kPa and 2.5Hz.

**movie S6. The simulated process of the assembly and actuation of the HCM and pneumatic HCM.** The dimensions for both models are $t$ = 0.381 mm, $\theta$ = 10˚, and $\gamma_s$ = 6.

**movie S7. The circular swimming of the motor-driven HCM fish in a lake.** The shape factors of the fish HCM are $\theta = -23.5$˚ and $\gamma_s$ = 2, and the undulation frequency is 3 Hz, yielding an average speed of 2.03 BL/s (43.6 cm/s).

**movie S8. The undulation of the untethered fish robot in the air and underwater.** The HCM used in the robot has shape factors $\theta = -23.5$˚ and $\gamma_s$ = 2. An average acceleration of 20.1 $cm/s^2$ is observed in the starting stage of the robotic straight swimming in the aquarium.

**movie S9. The high-frequency undulation of the motor-driven fish.** The shape factors of the fish HCM are $\theta = -23.5$˚ and $\gamma_s$ = 2, and the frequencies of the swinging are 2.5, 3.0, 3.5, and 4.0 Hz.